

Breakdown of thalamo-cortical connectivity precedes spike generation in focal epilepsies

Vitalie Chiosa, Stanislav A. Groppa, Dumitru Ciolac, Nabin Koirala, Liudmila Mişina, Yaroslav Winter, Maria Moldovanu, Muthuraman Muthuraman, Sergiu Groppa

Angaben zur Veröffentlichung / Publication details:

Chiosa, Vitalie, Stanislav A. Groppa, Dumitru Ciolac, Nabin Koirala, Liudmila Mişina, Yaroslav Winter, Maria Moldovanu, Muthuraman Muthuraman, and Sergiu Groppa. 2017. "Breakdown of thalamo-cortical connectivity precedes spike generation in focal epilepsies." *Brain Connectivity* 7 (5): 309-20.
<https://doi.org/10.1089/brain.2017.0487>.

Breakdown of thalamo-cortical connectivity precedes spike generation in focal epilepsies

Chiosa V^{1,2,3}, Groppa SA^{2,3}, Ciolac D^{1,2,3}, Koirala N¹, Mişina L^{2,3}, Winter Y¹, Moldovanu M⁴, Muthuraman M^{1*}, Groppa S^{1*}

¹Department of Neurology, Neuroimaging and Neurostimulation, Focus Program Translational Neuroscience (FTN), Rhine-Main Neuroscience Network (rmn²), University Medical Center of the Johannes Gutenberg University Mainz, Mainz, Germany.

²Department of Neurology and Neurosurgery, National Center of Epileptology, Institute of Emergency Medicine, Chisinau, Moldova.

³Laboratory of Neurobiology and Medical Genetics, State University of Medicine and Pharmacy “Nicolae Testemiţanu”, Chisinau, Moldova.

⁴German Diagnostic Center, Chisinau, Moldova.

*authors contributed equally

Short title: Connectivity changes before spike initiation

Corresponding author:

Prof. Dr. med. Sergiu Groppa

Neuroimaging and Neurostimulation,

Department of Neurology, Focus Program Translational Neuroscience (FTN), Rhine-Main

Neuroscience Network (rmn²)

Johannes Gutenberg University Mainz

Langenbeckstr.1, 55131 Mainz, Germany

Tel: +49-6131-17 7156; Fax: +49-6131-17 5697

E-mail: segroppa@uni-mainz.de

Key words: focal epilepsy, effective connectivity, spike generation, thalamo-cortical connections.

Abstract

EEG spikes and focal epileptic seizures are generated in circumscribed cerebral networks that have been insufficiently described. For precise time and spatial domain networks characterization we applied in patients with focal epilepsy dense array 256-channel EEG recordings with causal connectivity estimation using time resolved partial directed coherence and 3T-MRI derived cortical and thalamus integrity reconstruction. Prior to spike generation significant theta and alpha bands driven information flows alterations were noted from both temporal and frontal lobes to thalamus and from thalamus to the frontal lobe. Medial dorsal and ventral anterior nuclei of the thalamus were delimited as possible pacemakers. Markedly reduced thalamic volumes and impaired cortical integrity in widespread areas predicted the altered information flows. Our data reveal distinct patterns of connectivity involving the thalamus and frontal cortex directly and causally involved in spike generation. These structures might play an essential role for epileptogenesis and could be targeted in future therapeutic approaches.

Introduction

Focal epileptogenesis relies on perturbations of neuronal activity regionally and in a network of interconnected anatomical regions. Modified excitatory/inhibitory interactions within cortico-cortical or subcortical networks potentiate the local activity, generating long-range synchronizations. Pathologic synchronization could lead to interictal spikes, which are bursts of action potentials generated by recurrent excitation, followed by a period of inhibition (McCormick and Contreras 2001). This synchronization of electric activities recorded non-invasively is therefore an essential phenomenon that could help to resolve epileptogenic networks (Bartolomei, Wendling et al. 2001, de Curtis and Avanzini 2001). Recent studies investigating pathological synchronous neuronal activity and its structural correlates have led to a paradigm shift from “epileptogenic focus” to “epileptogenic network” (Siniatchkin, Groppa et al. 2007, Richardson 2012, Yaffe, Borger et al. 2015). One of the remote structures of the epileptogenic networks that is involved early in the temporal and spatial synchronization leading to seizure generation might be the thalamus; however its precise role in the propagation of focal seizures is not clear (Rosenberg, Mauguière et al. 2006, Groppa, Siebner et al. 2008, Groppa, Moeller et al. 2012). The thalamus as a network node not only receives substantial neuronal input from different brain regions, but has also strong reciprocal connections to other subcortical and cortical areas (Groppa, Siebner et al. 2008, Groppa, Moeller et al. 2012). Insausti *et al.* (Insausti, Amaral et al. 1987) showed that the mediodorsal nucleus (MD) of the thalamus has rich reciprocal interconnections with neocortical areas, such as with frontal and prefrontal cortex through anterior thalamic peduncle (Tanaka 1976) and with temporal regions like amygdala and olfactory cortex (Russchen, Amaral et al. 1987) through inferior thalamic peduncle. These pathways might be of special importance for seizure generation. As shown recently (Guye, Régis et al. 2006, Mueller, Laxer et al. 2010, Bernhardt, Bernasconi et al. 2012), the thalamus might also be involved in the long-range coupling in temporal lobe epilepsy (TLE), the most common type of focal epilepsy. However, it is still not known which thalamic subregions in humans modulate the information flows related to epileptogenesis and which frequency bands are involved. For the development of new therapeutic techniques such as invasive or non-invasive stimulation or neurosurgical methods, it is of utmost importance to characterize these functional and structural

abnormalities and describe the entire network involved (Groppa, Herzog et al. 2014, Muthuraman, Groppa et al. 2016). In the adopted approach of structural and functional network characterization we aimed to obtain an exact and causal estimation of the temporal and spatial properties of the involved networks. Moreover, the adopted approach describes the directionality of the information flows and achieves an exact temporal dissection of the connectivity dynamics. The proposed frequency domain analysis has a unique feature to describe time- and space-specific processes linked to distinct frequency bands that drive the long-range connectivity.

We hypothesize (1) frequency- and time domain-specific changes in connectivity prior to spike generation and (2) clear structural abnormalities involving the epileptogenic network that are related to the long-range synchronization and not solely to the primary focus.

Methods

Ethics statement. The study protocol was approved by the local ethical board at National Center of Epileptology institutional review board, Chisinau, Moldova.

Participants. 15 patients (mean age \pm standard deviation: 28.1 ± 8.3 years, 9 males) with focal epilepsy (12 TLE patients) without seizures in the month prior to investigation and 15 age-matched healthy subjects (27.9 ± 4.0 years, 7 males) were included. The diagnosis of epilepsy was established on the basis of clinical history and EEG findings according to revised International League Against Epilepsy (ILAE) classification (Berg, Berkovic et al. 2010). The recruited patients were referred to the National Center of Epileptology, Chisinau, Moldova. The demographic and clinical characteristics of each patient are summarized in Table 1. The analysis pipeline is presented in Figure 1.

EEG data acquisition. We performed interictal dense array video-EEG of epilepsy patients at rest and in an alert state for 2 hours in a dimly lit and quite room. The EEG electrodes were included in a cap with 20-25 mm interelectrode distances placed according to the international 10/5 system (Jurcak, Tsuzuki et al. 2007) (Hydrogel Geodesic Sensor Net 130 routine, 256 electrodes, Electrical Geodesic, Inc., Eugene, OR, USA). The sampling rate was 1000 Hz, with low and high frequency filters (0.3 Hz and 70 Hz, respectively) and stored using Net Station 5 software package (Electrical Geodesic). The obtained electrodes' impedance was below 10 k Ω . All patients were under continuous observation throughout the recording.

MRI data acquisition. Structural MR data were acquired using a 3T SIEMENS Skyra scanner, with a 32-channel head coil (Wellmer, Quesada et al. 2013). T1-weighted images (repetition time [TR] = 2000 msec, echo time [TE] = 9 msec, 4 mm slice thickness, flip angle = 150°), T2-weighted images (TR = 3800 msec, TE = 117 msec, 4 mm slice thickness, flip angle = 190°) and fluid attenuated inversion recovery (FLAIR) sequences were acquired.

Data Processing. EEG preprocessing and analysis was performed using FieldTrip toolbox and in-house Matlab scripts. Muscle artifacts were first removed using manual data inspection by an experienced neurophysiologist. An infomax Independent Component

Analysis (ICA) (Delorme and Makeig 2004) was then applied and ICA components were profiled by their topography, activation time course and spectrogram. Components clearly assigned to e.g., (rarely occurring) eye blinks (Jung, Makeig et al. 2000) were excluded from the back projection. EEG from all scalp channels were then transformed to the average reference (Lehmann and Skrandies 1980) and EEG segments with remaining artifacts were removed. Typical interictal spikes with the same morphology were marked manually at the time of maximum positivity or negativity, the detected spikes were checked individually, and some were excluded. In train interictal events like polyspikes or spikes riding on a preceding slow wave were also rejected in order to avoid pre-onset baseline contamination. For each patient 5-10 interictal spikes were selected. The EEG signal was parsed 15 seconds before the spike peak for each patient separately. The time interval of 10 seconds before the spike was defined as the activation period and the time period from 10 to 15 seconds before the spike was defined as the baseline period for all the following analyses. Source power and synchronization analysis (see below) across all sources was examined at theta (4–7 Hz), alpha (8–13 Hz) and beta (14–30 Hz) frequency bands separately.

Source analysis

A full description of the coherence analysis is given elsewhere (Muthuraman, Heute et al. 2012, Michels, Muthuraman et al. 2013). There are two major constraints in this analysis: first, the analysis is created on a single dipole model, which is not linearly correlated to other dipoles and second, the signal-to-noise ratio must be sufficiently high (Groß, Kujala et al. 2001). The fixed dipole model was used in which the dipole source responsible for the measured EEG potentials during an epoch remains at a constant location, the dipole moment vector maintains a constant orientation throughout the epoch, and only the magnitude varies. The output of the beamformer at a voxel in the brain can be defined as a weighted sum of the output of all EEG channels (Van Veen, Van Dronkelen et al. 1997). The weights determine the spatial filtering characteristics of the beamformer and are selected to increase the sensitivity to signals from a voxel and reduce the contributions of signals from (noise) sources at different locations. The frequency components and their linear interaction are represented as a cross-spectral density (CSD) matrix. In order to

visualize power at a given frequency range, a linear transformation was used based on a constrained optimization problem, which acts as a spatial filter (Van Veen, Van Drongelen et al. 1997). The spatial filter was applied to a large number of voxels covering the entire brain, assigning a specific value of power to each voxel. A voxel size of 5 mm was used in this study. The beamformer weights for a given source (at a location of interest) are determined by the data covariance matrix and the forward-solution (lead-field matrix - LFM). The LFM was estimated with specified models for the brain. In this study, the brain was modeled by a boundary element method (Fuchs, Kastner et al. 2002) with three layers, namely brain, skull and skin. The volume conductor model was created using individual T1 magnetic resonance images. Part of the forward modeling and the source analysis were done using the open source software FieldTrip (Oostenveld, Fries et al. 2010). For both groups, the head was modeled using the individual electrode locations. The LFM contains information about the geometry and conductivity of the model. The complete description of the solution for the forward problem has been described previously (Muthuraman, Heute et al. 2010). The brain regions were defined according to the Automatic Anatomic Labeling Atlas (AAL) 116 regions of interest (ROIs) (Whitfield-Gabrieli and Nieto-Castanon 2012). To address major anatomically relevant regions, the ROIs were subdivided into seven separate regions, namely prefrontal, frontal, parietal, occipital, temporal, thalamus and cerebellum. The thalamus parcellation was done based on the connectivity probability to cortical masks (Behrens, Johansen-Berg et al. 2003, Jones 2012). The activated voxels were selected by a within-subject surrogate analysis to define the significance level, which was then used to identify voxels in the regions as activated voxels. Once brain region voxels were identified, their activity was extracted from the surface EEG (source space). In a further analysis, all the original source signals for each region with several activated voxels were combined by estimating the second order spectra and employing a weighting scheme depending on the analyzed frequency range to form a pooled source signal estimate for each region as previously described (Rosenberg, Amjad et al. 1989, Amjad, Halliday et al. 1997).

Connectivity analysis

Using time-frequency causality we can not only focus on a particular frequency, but can also analyze the time-dynamics of the causality at that frequency. Based on the state-space modeling, the time-frequency causality estimation method of time-resolved partial directed coherence (TPDC) utilizes dual-extended Kalman filtering (DEKF) (Haykin 2001, Wan and Nelson 2001). We can estimate the time-varying dependent autoregressive (AR) coefficients. One extended Kalman Filter (EKF) will estimate the states and feed this information to the other EKF; the second EKF will estimate the model parameters and will also share this information with the first EKF. By concurrently using two Kalman filters, working in parallel with one another, we can estimate both states and model parameters of the system at each time instance. After estimating the time-varying multivariate (MVAR) coefficients, the next step is to use those coefficients for the calculation of causality between the time series. Since DEKF can give us the time-varying MVAR coefficients at each time point, we can calculate the partial directed coherence (PDC) at each time point as well. The general expression for the PDC is given as follows:

$$|\pi_{i \leftarrow j}(\omega)| = \frac{|A_{ij}(\omega)|}{\sqrt{\sum_k |A_{kj}(\omega)|^2}} \quad (1)$$

In equation (1), π is the magnitude of PDC from time series j to i at frequency ω , which are the Fourier transform coefficients of the causal coefficients. Afterwards, time-frequency plots of all PDCs can be concatenated to produce a single time-frequency plot. The precise distribution of the MVAR coefficients is not known; we used the surrogate method to check for the significance of the results. This method is based on the random shuffling of the subjected time series and hence it is data-driven. In short, we divided the original time series into smaller non-overlapping windows and randomly shuffled the order of these windows to create a new time series. The MVAR model is fitted to this shuffled time series and the TPDC is estimated. This process is repeated 100 times and the average TPDC is calculated. The resulting value is the significance threshold value for all our connections. This process is performed separately for each patient.

The mean TPDC values for the significant connections from the different time windows were compared with a repeated-measure ANOVA. The significance level was set to $p < 0.05$. Post-hoc tests with Tukey-Kramer correction for multiple comparisons were applied.

Cortical thickness analysis

Cortical reconstruction and volumetric segmentation were performed with the Freesurfer image analysis suite (version 5.3.0), which is documented and freely available for download online (<http://surfer.nmr.mgh.harvard.edu/>). The detailed procedure for surface and volumetric reconstruction has been described and validated in previous studies (Dale, Fischl et al. 1999, Fischl and Dale 2000, Reuter, Schmansky et al. 2012). In brief, cortical thickness was calculated (in mm) as the shortest distance between grey matter/white matter boundary and pial surface across the cortical mantle. Thalamus volume was calculated using the automated procedure and checked visually. Cortical thickness was smoothed with a 10-mm full width at half height Gaussian kernel to reduce local variations in the measurements (Du, Schuff et al. 2007). Statistical difference was computed using a random effects model with t-tests for each cortical location. For statistical difference maps the significant threshold was set to an uncorrected p-value of $p < 0.05$ (two-tailed) (Lyo, Sung et al. 2006).

In order to relate information flow changes and structure we computed the difference ($\nabla = \max_{Tpdc} - \min_{Tpdc}$) in connectivity dynamics prior to spike generation and cortical thickness and thalamic volume values.

Results

Clinical description

In this study, a total of 15 epilepsy patients and 15 age-matched healthy controls were analyzed. The healthy controls did not present any history of seizures or other neurologic abnormalities. There was no significant difference in age ($p > 0.05$) between the two cohorts. All patients except one were right handed. Thirteen patients had dyscognitive seizures and three patients presented focal motor seizures with evolution in bilateral convulsive seizures. Among 15 patients, the radiological MRI assessment showed no

morphological correlate in one case, the others presented different structural lesions (see Table 1).

Temporal dynamics of effective connectivity

The analysis of the focused frequency bands (theta, alpha and beta) in the period prior to spike generation showed significant information flows only in theta ($t = 4.06$, $p = 0.005$) and alpha ($t = 4.36$, $p = 0.003$) frequency bands. These survived the data driven surrogate significance analysis and will be discussed further in this section.

In patients we detect a significant decrease in connectivity strength from temporal and frontal lobes to thalamus and from thalamus to the frontal lobe in the theta domain with a maximum peak five seconds prior to spike generation (Figure 2a). Moreover, just prior to spike appearance (in the last four seconds) the connectivity from the temporal lobe to thalamus increases significantly. Furthermore, we see a similar pattern of connectivity dynamics in the alpha band (Figure 2b). Here, we see a clear information flow increase from temporal lobe to thalamus that also peaks five seconds prior to spike generation. A further significant breakdown of information flows between the temporal and frontal lobe to thalamus was noted.

The strength of temporo-thalamic connectivity change (five seconds prior to spike) significantly correlated with fronto-thalamic connectivity dynamics ($r = 0.73$, $p = 0.001$). In the same band and time window, the thalamo-frontal connectivity values showed no significant interrelations with temporo-thalamic ($p = 0.06$) and fronto-thalamic ($p = 0.5$) connectivity variations.

In the alpha band, thalamo-frontal connectivity correlated significantly with the modulation of fronto-thalamic ($r = 0.63$, $p = 0.01$) and not significantly with the temporo-thalamic ($p = 0.7$) information flows. Temporo-thalamic connectivity also did not correlate with the fronto-thalamic connectivity dynamics ($p = 0.5$).

No other significant changes of connectivity were noted between the further analyzed cerebral regions (i.e., occipital, parietal, prefrontal).

In healthy subjects for the analyzed frequency bands (theta, alpha and beta) we found significant information flows only in alpha frequency band. Bidirectional connections were attested between frontal lobe and thalamus ($t = 4.01$, $p = 0.006$) and between frontal and

parietal lobes ($t = 4.16$, $p = 0.004$) that survived the data driven surrogate significance analysis. In the analyzed time window of 10 seconds, no significant changes in information flows were detected for these connections, which were stable over the entire time interval.

Thalamic parcellation related connectivity dynamics

In the theta frequency band, we found significant bidirectional connections from the medial dorsal and ventral anterior thalamus to the frontal lobe (Figure 3). The temporal dynamics of connectivity changes were similar to the above described changes of connectivity involving the entire thalamus structure. In the alpha frequency band we see a similar breakdown of the connectivity strength involving the frontal lobe and the medial dorsal and ventral anterior nuclei of the thalamus. A significant reduction in information flows was detected ca. 5 seconds before spike generation from temporal lobe to the anterior, lateral and inferior nuclei of pulvinar of thalamus as shown in Figures 5 and 6.

Cortical thickness and thalamic volume

Cortical thickness analysis showed a significant cortical thinning of wide spread regions in patients with epilepsy ($p < 0.05$, FDR [false discovery rate] corrected; > 50 voxels) mainly in the frontal and temporal regions (Figure 7). A cortical thickness increase was detected in the occipital cortex. The complete results are presented in Table 2 and Figure 7. No significant correlations were found between cortical thickness and disease duration.

Thalamic volumes were markedly reduced in epilepsy patients compared to healthy subjects. Volumes of left ($7362.1 \pm 848.3 \text{ mm}^3$, $p = 0.00005$) and right ($7186 \pm 848.3 \text{ mm}^3$, $p = 0.0037$) thalami of FE patients were significantly smaller in comparison with healthy controls (left thalamus $9360.5 \pm 1382 \text{ mm}^3$, right thalamus $8088.7 \pm 683 \text{ mm}^3$).

Correlation effective connectivity and thalamic volume

In theta band the temporo-thalamic effective connectivity significantly correlated with the volumes of both thalami ($r = 0.8981$, $p < 0.001$), while fronto-thalamic connectivity did not show significant correlations with the thalamic volumes ($p > 0.1$) or only a trend for the thalamo-frontal connection ($r = -0.5$, $p = 0.058$). In the alpha band, only fronto-thalamic effective connectivity significantly correlated with the volumes of both thalami ($r = -0.61$,

$p < 0.01$); while the correlations between temporo-thalamic and thalamo-frontal effective connectivities and thalamic volumes did not reach statistical significance ($p > 0.1$ and $p > 0.5$ respectively).

Discussion

In this work, we analyze information flows and structural integrity as network fingerprints of the circuits that drive the spike generation and seizure evolution. Establishing the directionality and the causality of cerebral dynamics is essential for linking network connectivity and seizure prediction. Therefore, we investigated non-invasively the alterations of effective connectivity in a group of patients with focal epilepsy during the interictal period and specifically focused on the narrow time period prior to spike appearance on scalp EEG. Moreover, we dissected the cortical and subcortical integrity within these networks that modulate the long-range information flows and synchronizations. We see clear connectivity alterations in the theta and alpha bands before spike generation. Our analysis addressed bidirectional information flows among cortical regions and thalamus. Significant information flows were detected in a network formed by temporal and frontal cortices and thalamus. The performed analyses demonstrate a clear breakdown of connectivity patterns five seconds prior to spike generation with a subsequent increase. Medial dorsal and ventral anterior nuclei of the thalamus were mainly involved. Widespread cortical integrity abnormalities and thalamic atrophy were attested in the patient group.

Frequency band specificity

The main effective connectivity variations were identified in theta and alpha bands. A clear physiological framework explains our results. Theta oscillations synchronize mesial temporal lobe (MTL) with distant cortical and subcortical regions (Zaveri, Duckrow et al. 2001, Bettus, Wendling et al. 2008), while pathological synchronization phenomena involving MTL could be as well mirrored in this frequency band. The underlying cause of these connectivity alterations has not yet been described. One putative explanation could be that the breakdown of effective connectivity from temporal and frontal lobes towards the thalamus in theta band is caused by an altered physiological synchronization. The state of decreased synchronization could lead to vulnerability to following information flows increasing the probability of spikes or seizures (Mormann, Kreuz et al. 2003). Consequently, we see an increase of information flows in the temporo-thalamic connections thereafter.

A recent study investigating information flows in patients with TLE by the aid of EEG-functional fMRI analysis (Faizo, Burianová et al. 2014) showed similarly significant reductions in information flows before spike occurrence. A decreased connectivity between both temporal lobes has been attested prior to spike generation. Summated, it can be postulated that putative breakdowns of information flows in the involved structures lead to vulnerable states of decreased synchronization that can drive epileptogenesis.

Region specificity

In our study, we see a direct involvement of thalamus, temporal and frontal lobes, sparing occipital and parietal cortices and other studied areas. The described information flows involving thalamus utilizes physiological circuits. Different thalamic nuclei are involved and modulate long-range synchronizations at distinct frequency bands (Wang 2010). Anterior thalamus is involved in theta synchronization, while pulvinar is responsible for alpha driven information flows (Ketz, Jensen et al. 2015). Through theta synchronization anterior thalamus modulates the information flows between hippocampus and medial prefrontal cortex (PFC), while pulvinar nuclei synchronize parietal and visual cortex with medial, lateral and orbital PFC within alpha band (Ketz, Jensen et al. 2015). In our analysis relating to thalamic nuclei and temporo-thalamo-frontal connections, anterior nucleus of thalamus displayed significant alterations of effective connectivity in theta and alpha ranges, while medial dorsal nucleus showed long-range synchronizations in theta and alpha bands, but not in beta. Lateral and inferior nuclei of pulvinar showed a connectivity increase in theta and a decrease in alpha synchronization range.

The described connectivity dynamics show some similarities to known network determinants in generalized epilepsies. In this type of epilepsies fronto-thalamic synchronizations are a typical hallmarks of very early absence seizure activity as evidenced by EEG and MEG (Holmes, Brown et al. 2004, Groppa, Siebner et al. 2008, Groppa, Moeller et al. 2012, Tenney, Fujiwara et al. 2013). Disruptions of synchrony-limiting mechanisms in thalamus might lead to hypersynchrony with cortical areas and predispose to spike-wave discharges and absence seizures (Paz, Bryant et al. 2011).

Some of the regions identified in our study like medial temporal and frontal lobes are a part of the so called default mode network (DMN). Studies analyzing structural and

functional connectivity abnormalities within medial temporal lobe and DMN brain areas with (Pittau, Grova et al. 2012, Kay, DiFrancesco et al. 2013) or without (Morgan, Sonmezturk et al. 2012, Voets, Beckmann et al. 2012) simultaneous EEG recording suggest the presence of important disconnections in DMN sites in TLE patients. Moreover, interictal discharges might be associated with significant deactivation in default mode brain areas (Laufs, Hamandi et al. 2007).

In the comparison of grey matter structural integrity between patients and healthy controls, we depict wide spread areas in the temporal and fronal regions but also parietal and prefrontal cortex, suggesting a putative relation to long-range synchronization and connectivity breakdown. However, cortical thinning was more evident in the neocortical regions. Cortical changes within distant regions, like frontal or parietal cortex could be related to the effects of persistent changed connectivity flows, appearing epileptiform discharges or seizures (Keller, Mackay et al. 2002, Lin, Salamon et al. 2007). Our patients showed bilateral thinning of sensorimotor regions; while the reasons for these changes still need to be clarified, one possible explanation could play the modified information flows between thalamus and frontal areas with subsequent cortico-cortical connections to the sensorimotor cortex. The fact that pre- and postcentral cortical thinning is mentioned in studies assessing cortical thickness in TLE (Lin, Salamon et al. 2007, Bernhardt, Worsley et al. 2008), suggests that these regions are directly involved in the focal epileptogenesis.

Thalamic volume and connectivity

Thalamus might be one of most strongly affected region of extratemporal grey matter in patients with focal epilepsies (Barron, Fox et al. 2013), while its role for seizure propagation is still unclear (Cassidy and Gale 1998, Guye, Régis et al. 2006). In our study thalamic volumes showed bilateral reductions and a strong negative correlation between the duration of epilepsy and volumetric values. Of particular interest is the significant relationship between temporo-thalamic cross-talk in theta frequency band and fronto-thalamic connectivity in alpha frequency bands and the volume of both thalami.

Thalamic regions most commonly associated with TLE are pulvinar, anterior nucleus, and medial dorsal nucleus (Barron, Fox et al. 2013), which have dense reciprocal connections with MTL. Volume loss in all three nuclei has been correlated with duration and severity of

medial TLE (Bernhardt, Bernasconi et al. 2012), further supporting their conspicuous involvement in the epileptogenic network. The pulvinar part of the thalamus has several nuclear subgroups and the most medial–dorsal part is connected to associative cortices of the frontal and temporal lobes (Rosenberg, Mauguière et al. 2006). Extensive and reciprocal interconnections with the cortex implies that pulvinar serves in facilitation of cortico-cortical transmission through thalamic loops (Saalman and Kastner 2011). Local pulvinar subnetworks receiving strong extrathalamic excitatory and inhibitory inputs are more susceptible to rhythmic bursting and respectively to integration into remote oscillations (Wei, Bonjean et al. 2011, Fogerson and Huguenard 2016). The nuclear subgroups identified in our study were medial dorsal and ventral anterior nuclei with frontal projections, and lateral and inferior nuclei of pulvinar with temporal connections which are in a very good agreement with existing data (Behrens, Johansen-Berg et al. 2003, Bernhardt, Bernasconi et al. 2012). Therefore it is of high importance to reveal and characterize the contributions of extrathalamic associated cortices to initiation and generalization of hypersynchronous oscillations in thalamic nuclei (Fogerson and Huguenard 2016).

Different nuclei of thalamus might have specific roles in temporo-thalamic epileptogenic synchronization. The anterior nucleus of thalamus projects to superior frontal and temporal lobe structures and bilateral stimulation of this nucleus reduces seizure frequency (Fisher, Salanova et al. 2010), thus displaying an essential modulatory role in focal epileptogenesis. Quick generalization of seizures stimulated from medial dorsal nucleus of thalamus implies this region the role in spreading of TLE seizures (Bertram, Zhang et al. 2008).

Conclusions

Our combined approach of connectivity and microstructural integrity analysis of focal epileptogenic networks identified the temporal and spatial domain specificity and the frequency spectrum of synchronization leading to spikes. These networks involving the temporal and frontal cortical areas and thalamus are hallmarks of interictal pathological activity generation utilizing mostly physiological connection but leading to a spread to adjacent regions forming the epileptogenic network. Our findings offer clear insights into

the function and structure of brain networks underlying the genesis of spikes and seizures in focal epilepsy and can be possibly targeted by future therapeutic strategies.

Acknowledgements

The authors thank Cheryl Ernest for proofreading the manuscript. This work was supported by a grant from the German Research Council (DFG; CRC-1193/B5 and TR-128 to SG). The funders had no role in study design, data collection and analysis, decision to publish, or preparation of the manuscript.

Disclosure statement

None of the authors have any conflict of interest to disclose. No competing financial interests exist. We confirm that we have read the Journal's position on issues involved in ethical publication and affirm that this report is consistent with those guidelines.

References:

- Amjad, A., D. Halliday, J. Rosenberg and B. Conway (1997). "An extended difference of coherence test for comparing and combining several independent coherence estimates: theory and application to the study of motor units and physiological tremor." Journal of neuroscience methods **73**(1): 69-79.
- Barron, D. S., P. M. Fox, A. R. Laird, J. L. Robinson and P. T. Fox (2013). "Thalamic medial dorsal nucleus atrophy in medial temporal lobe epilepsy: a VBM meta-analysis." Neuroimage: Clinical **2**: 25-32.
- Bartolomei, F., F. Wendling, J.-J. Bellanger, J. Régis and P. Chauvel (2001). "Neural networks involving the medial temporal structures in temporal lobe epilepsy." Clinical neurophysiology **112**(9): 1746-1760.
- Behrens, T., H. Johansen-Berg, M. Woolrich, S. Smith, C. Wheeler-Kingshott, P. Boulby, G. Barker, E. Sillery, K. Sheehan and O. Ciccarelli (2003). "Non-invasive mapping of connections between human thalamus and cortex using diffusion imaging." Nature neuroscience **6**(7): 750-757.
- Berg, A. T., S. F. Berkovic, M. J. Brodie, J. Buchhalter, J. H. Cross, W. van Emde Boas, J. Engel, J. French, T. A. Glauser and G. W. Mathern (2010). "Revised terminology and concepts for organization of seizures and epilepsies: report of the ILAE Commission on Classification and Terminology, 2005–2009." Epilepsia **51**(4): 676-685.
- Bernhardt, B. C., N. Bernasconi, H. Kim and A. Bernasconi (2012). "Mapping thalamocortical network pathology in temporal lobe epilepsy." Neurology **78**(2): 129-136.
- Bernhardt, B. C., K. J. Worsley, P. Besson, L. Concha, J. P. Lerch, A. C. Evans and N. Bernasconi (2008). "Mapping limbic network organization in temporal lobe epilepsy using morphometric correlations: insights on the relation between mesiotemporal connectivity and cortical atrophy." Neuroimage **42**(2): 515-524.
- Bertram, E. H., D. Zhang and J. M. Williamson (2008). "Multiple roles of midline dorsal thalamic nuclei in induction and spread of limbic seizures." Epilepsia **49**(2): 256-268.
- Bettus, G., F. Wendling, M. Guye, L. Valton, J. Régis, P. Chauvel and F. Bartolomei (2008). "Enhanced EEG functional connectivity in mesial temporal lobe epilepsy." Epilepsy research **81**(1): 58-68.

- Cassidy, R. M. and K. Gale (1998). "Mediodorsal thalamus plays a critical role in the development of limbic motor seizures." The Journal of neuroscience **18**(21): 9002-9009.
- Dale, A. M., B. Fischl and M. I. Sereno (1999). "Cortical surface-based analysis. I. Segmentation and surface reconstruction." Neuroimage **9**(2): 179-194.
- de Curtis, M. and G. Avanzini (2001). "Interictal spikes in focal epileptogenesis." Progress in neurobiology **63**(5): 541-567.
- Delorme, A. and S. Makeig (2004). "EEGLAB: an open source toolbox for analysis of single-trial EEG dynamics including independent component analysis." Journal of neuroscience methods **134**(1): 9-21.
- Du, A.-T., N. Schuff, J. H. Kramer, H. J. Rosen, M. L. Gorno-Tempini, K. Rankin, B. L. Miller and M. W. Weiner (2007). "Different regional patterns of cortical thinning in Alzheimer's disease and frontotemporal dementia." Brain **130**(4): 1159-1166.
- Faizo, N. L., H. Burianová, M. Gray, J. Hocking, G. Galloway and D. Reutens (2014). "Identification of Pre-Spike Network in Patients with Mesial Temporal Lobe Epilepsy." Frontiers in Neurology **5**: 222.
- Fischl, B. and A. M. Dale (2000). "Measuring the thickness of the human cerebral cortex from magnetic resonance images." Proceedings of the National Academy of Sciences **97**(20): 11050-11055.
- Fisher, R., V. Salanova, T. Witt, R. Worth, T. Henry, R. Gross, K. Oommen, I. Osorio, J. Nazzaro and D. Labar (2010). "Electrical stimulation of the anterior nucleus of thalamus for treatment of refractory epilepsy." Epilepsia **51**(5): 899-908.
- Fogerson, P. M. and John R. Huguenard (2016). "Tapping the Brakes: Cellular and Synaptic Mechanisms that Regulate Thalamic Oscillations." Neuron **92**(4): 687-704.
- Fuchs, M., J. Kastner, M. Wagner, S. Hawes and J. S. Ebersole (2002). "A standardized boundary element method volume conductor model." Clinical Neurophysiology **113**(5): 702-712.
- Groppa, S., J. Herzog, D. Falk, C. Riedel, G. Deuschl and J. Volkmann (2014). "Physiological and anatomical decomposition of subthalamic neurostimulation effects in essential tremor." Brain **137**(1): 109-121.
- Groppa, S., F. Moeller, H. Siebner, S. Wolff, C. Riedel, G. Deuschl, U. Stephani and M. Siniatchkin (2012). "White matter microstructural changes of thalamocortical networks in

- photosensitivity and idiopathic generalized epilepsy." Epilepsia **53**(4): 668-676.
- Groppa, S., H. R. Siebner, C. Kurth, U. Stephani and M. Siniatchkin (2008). "Abnormal response of motor cortex to photic stimulation in idiopathic generalized epilepsy." Epilepsia **49**(12): 2022-2029.
- Groß, J., J. Kujala, M. Hämäläinen, L. Timmermann, A. Schnitzler and R. Salmelin (2001). "Dynamic imaging of coherent sources: studying neural interactions in the human brain." Proceedings of the National Academy of Sciences **98**(2): 694-699.
- Guye, M., J. Régis, M. Tamura, F. Wendling, A. Mc Gonigal, P. Chauvel and F. Bartolomei (2006). "The role of corticothalamic coupling in human temporal lobe epilepsy." Brain **129**(7): 1917-1928.
- Haykin, S. S. (2001). Kalman filtering and neural networks, Wiley Online Library.
- Holmes, M. D., M. Brown and D. M. Tucker (2004). "Are "generalized" seizures truly generalized? Evidence of localized mesial frontal and frontopolar discharges in absence." Epilepsia **45**(12): 1568-1579.
- Insausti, R., D. Amaral and W. Cowan (1987). "The entorhinal cortex of the monkey: III. Subcortical afferents." Journal of Comparative Neurology **264**(3): 396-408.
- Jones, E. G. (2012). The thalamus, Springer Science & Business Media.
- Jung, T.-P., S. Makeig, C. Humphries, T.-W. Lee, M. J. Mckeown, V. Iragui and T. J. Sejnowski (2000). "Removing electroencephalographic artifacts by blind source separation." Psychophysiology **37**(02): 163-178.
- Jurcak, V., D. Tsuzuki and I. Dan (2007). "10/20, 10/10, and 10/5 systems revisited: their validity as relative head-surface-based positioning systems." Neuroimage **34**(4): 1600-1611.
- Kay, B. P., M. W. DiFrancesco, M. D. Privitera, J. Gotman, S. K. Holland and J. P. Szaflarski (2013). "Reduced default mode network connectivity in treatment-resistant idiopathic generalized epilepsy." Epilepsia **54**(3): 461-470.
- Keller, S. S., C. E. Mackay, T. R. Barrick, U. C. Wieshmann, M. A. Howard and N. Roberts (2002). "Voxel-based morphometric comparison of hippocampal and extrahippocampal abnormalities in patients with left and right hippocampal atrophy." Neuroimage **16**(1): 23-31.
- Ketz, N. A., O. Jensen and R. C. O'Reilly (2015). "Thalamic pathways underlying prefrontal

- cortex–medial temporal lobe oscillatory interactions." Trends in neurosciences **38**(1): 3-12.
- Laufs, H., K. Hamandi, A. Salek-Haddadi, A. K. Kleinschmidt, J. S. Duncan and L. Lemieux (2007). "Temporal lobe interictal epileptic discharges affect cerebral activity in "default mode" brain regions." Human brain mapping **28**(10): 1023-1032.
- Lehmann, D. and W. Skrandies (1980). "Reference-free identification of components of checkerboard-evoked multichannel potential fields." Electroencephalography and clinical neurophysiology **48**(6): 609-621.
- Lin, J. J., N. Salamon, A. D. Lee, R. A. Dutton, J. A. Geaga, K. M. Hayashi, E. Luders, A. W. Toga, J. Engel and P. M. Thompson (2007). "Reduced neocortical thickness and complexity mapped in mesial temporal lobe epilepsy with hippocampal sclerosis." Cerebral cortex **17**(9).
- Lyoo, I. K., Y. H. Sung, S. R. Dager, S. D. Friedman, J. Y. Lee, S. J. Kim, N. Kim, D. L. Dunner and P. F. Renshaw (2006). "Regional cerebral cortical thinning in bipolar disorder." Bipolar disorders **8**(1): 65-74.
- McCormick, D. A. and D. Contreras (2001). "On the cellular and network bases of epileptic seizures." Annual review of physiology **63**(1): 815-846.
- Michels, L., M. Muthuraman, R. Lüchinger, E. Martin, A. R. Anwar, J. Raethjen, D. Brandeis and M. Siniatchkin (2013). "Developmental changes of functional and directed resting-state connectivities associated with neuronal oscillations in EEG." NeuroImage **81**: 231-242.
- Morgan, V. L., H. H. Sonmezturk, J. C. Gore and B. Abou-Khalil (2012). "Lateralization of temporal lobe epilepsy using resting functional magnetic resonance imaging connectivity of hippocampal networks." Epilepsia **53**(9): 1628-1635.
- Mormann, F., T. Kreuz, R. G. Andrzejak, P. David, K. Lehnertz and C. E. Elger (2003). "Epileptic seizures are preceded by a decrease in synchronization." Epilepsy research **53**(3): 173-185.
- Mueller, S. G., K. D. Laxer, J. Barakos, I. Cheong, D. Finlay, P. Garcia, V. Cardenas-Nicolson and M. W. Weiner (2010). "Involvement of the thalamocortical network in TLE with and without mesiotemporal sclerosis." Epilepsia **51**(8): 1436-1445.
- Muthuraman, M., S. Groppa and G. Deuschl (2016). "Cerebello-cortical networks in orthostatic tremor." Brain **139**(8): 2104-2106.
- Muthuraman, M., U. Heute, K. Arning, A. R. Anwar, R. Elble, G. Deuschl and J. Raethjen

- (2012). "Oscillating central motor networks in pathological tremors and voluntary movements. What makes the difference?" Neuroimage **60**(2): 1331-1339.
- Muthuraman, M., U. Heute, G. Deuschl and J. Raethjen (2010). The central oscillatory network of essential tremor. 2010 Annual International Conference of the IEEE Engineering in Medicine and Biology, IEEE.
- Oostenveld, R., P. Fries, E. Maris and J.-M. Schoffelen (2010). "FieldTrip: open source software for advanced analysis of MEG, EEG, and invasive electrophysiological data." Computational intelligence and neuroscience **2011**.
- Paz, J. T., A. S. Bryant, K. Peng, L. Fenno, O. Yizhar, W. N. Frankel, K. Deisseroth and J. R. Huguenard (2011). "A new mode of corticothalamic transmission revealed in the Gria4-/- model of absence epilepsy." Nature neuroscience **14**(9): 1167-1173.
- Pittau, F., C. Grova, F. Moeller, F. Dubeau and J. Gotman (2012). "Patterns of altered functional connectivity in mesial temporal lobe epilepsy." Epilepsia **53**(6): 1013-1023.
- Reuter, M., N. J. Schmansky, H. D. Rosas and B. Fischl (2012). "Within-subject template estimation for unbiased longitudinal image analysis." Neuroimage **61**(4): 1402-1418.
- Richardson, M. P. (2012). "Large scale brain models of epilepsy: dynamics meets connectomics." Journal of Neurology, Neurosurgery & Psychiatry **83**(12): 1238-1248.
- Rosenberg, D. S., F. Mauguière, G. Demarquay, P. Ryvlin, J. Isnard, C. Fischer, M. Guénot and M. Magnin (2006). "Involvement of medial pulvinar thalamic nucleus in human temporal lobe seizures." Epilepsia **47**(1): 98-107.
- Rosenberg, J., A. Amjad, P. Breeze, D. Brillinger and D. Halliday (1989). "The Fourier approach to the identification of functional coupling between neuronal spike trains." Progress in biophysics and molecular biology **53**(1): 1-31.
- Russchen, F., D. Amaral and J. Price (1987). "The afferent input to the magnocellular division of the mediodorsal thalamic nucleus in the monkey, *Macaca fascicularis*." Journal of Comparative Neurology **256**(2): 175-210.
- Saalmann, Y. B. and S. Kastner (2011). "Cognitive and Perceptual Functions of the Visual Thalamus." Neuron **71**(2): 209-223.
- Siniatchkin, M., S. Groppa, B. Jerosch, H. Muhle, C. Kurth, A. J. Shepherd, H. Siebner and U. Stephani (2007). "Spreading photoparoxysmal EEG response is associated with an abnormal cortical excitability pattern." Brain **130**(1): 78-87.

- Tanaka, D. (1976). "Thalamic projections of the dorsomedial prefrontal cortex in the rhesus monkey (*Macaca mulatta*)."
Brain research **110**(1): 21-38.
- Tenney, J. R., H. Fujiwara, P. S. Horn, S. E. Jacobson, T. A. Glauser and D. F. Rose (2013). "Focal corticothalamic sources during generalized absence seizures: a MEG study." Epilepsy research **106**(1): 113-122.
- Van Veen, B. D., W. Van Drongelen, M. Yuchtman and A. Suzuki (1997). "Localization of brain electrical activity via linearly constrained minimum variance spatial filtering." IEEE Transactions on biomedical engineering **44**(9): 867-880.
- Voets, N. L., C. F. Beckmann, D. M. Cole, S. Hong, A. Bernasconi and N. Bernasconi (2012). "Structural substrates for resting network disruption in temporal lobe epilepsy." Brain **135**(8): 2350-2357.
- Wan, E. A. and A. T. Nelson (2001). "Dual extended Kalman filter methods." Kalman filtering and neural networks: 123-173.
- Wang, X.-J. (2010). "Neurophysiological and computational principles of cortical rhythms in cognition." Physiological reviews **90**(3): 1195-1268.
- Wei, H., M. Bonjean, H. M. Petry, T. J. Sejnowski and M. E. Bickford (2011). "Thalamic burst firing propensity: a comparison of the dorsal lateral geniculate and pulvinar nuclei in the tree shrew." The Journal of neuroscience **31**(47): 17287-17299.
- Wellmer, J., C. M. Quesada, L. Rothe, C. E. Elger, C. G. Bien and H. Urbach (2013). "Proposal for a magnetic resonance imaging protocol for the detection of epileptogenic lesions at early outpatient stages." Epilepsia **54**(11): 1977-1987.
- Whitfield-Gabrieli, S. and A. Nieto-Castanon (2012). "Conn: a functional connectivity toolbox for correlated and anticorrelated brain networks." Brain connectivity **2**(3): 125-141.
- Yaffe, R. B., P. Borger, P. Megevand, D. M. Groppe, M. A. Kramer, C. J. Chu, S. Santaniello, C. Meisel, A. D. Mehta and S. V. Sarma (2015). "Physiology of functional and effective networks in epilepsy." Clinical Neurophysiology **126**(2): 227-236.
- Zaveri, H. P., R. B. Duckrow, N. C. De Lanerolle and S. S. Spencer (2001). "Distinguishing subtypes of temporal lobe epilepsy with background hippocampal activity." Epilepsia **42**(6): 725-730.

Tables:**Table 1.** Demographic, clinical and MRI data of epilepsy patients.

Patient No	Handedness	Age	Gender	Age at onset	Seizure type	MRI findings
1.	R	22	M	15	DS→BCS	Normal
2.	R	24	F	17	DS→BCS	R temporoparietal GMH
3.	R	14	M	6	DS→BCS	L MTS
4.	R	32	F	10	EMS→BCS	L MTS
5.	L	15	M	2	EMS→BCS	L parieto-occipital EM
6.	R	27	F	9	DS→BCS	R temporal glial scar
7.	R	26	M	12	DS→BCS	L temporal glial scars
8.	R	32	M	15	DS→BCS	Nonspecific WM lesions
9.	R	32	M	11	DS→BCS	L MTS
10.	R	22	F	13	DS→BCS	L MTS
11.	R	31	F	7	DS→BCS	R temporal subarachnoid cyst
12.	R	26	F	9	EMS→BCS	R MTS
13.	R	38	M	35	DS→BCS	Nonspecific WM lesions
14.	R	36	F	2	DS→BCS	L MTS
15.	R	45	M	41	DS→BCS	WM, L PHG foci of demyelination

R – right; **L** – left; **MRI** - magnetic resonance imaging; **DS** - dyscognitive seizures; **BCS** – bilateral convulsive seizures; **EMS** – elementary motor seizures; **GMH** - grey matter heterotopia; **MTS** - mesial temporal sclerosis; **WM** – white matter; **EM** – encephalomalacia; **PHG** –parahippocampal gyrus.

Table 2. Significant clusters derived from comparison between focal epilepsy patients and healthy controls, tabulated with the corresponding t-values, surface area (mm²) and Talairach coordinates.

Right hemisphere						
Cluster No	t-Max	Size (mm²)	Tal X	Tal Y	Tal Z	Annotation
1	-6.7544	1475.37	60.7	-41.4	17.4	supramarginal
2	-6.4630	412.76	58.1	-49.1	3.3	bankssts
3	-5.0150	820.58	62.1	-11.2	-22.2	middletemporal
4	-4.6995	307.02	52.7	6.6	-13.5	superiortemporal
5	-4.3071	272.79	29.7	6.1	-33.2	temporalpole
6	-4.2364	439.18	36.8	-0.9	-7.0	insula
7	3.9993	317.45	5.0	-84.6	9.5	cuneus
8	-3.9980	372.07	7.0	36.2	46.9	superiorfrontal
9	-3.8235	103.50	58.2	0.6	28.8	precentral
10	-3.6384	108.07	5.9	-36.0	2.0	posteriorcingulate
11	-3.4420	182.46	2.6	12.3	4.6	parsopercularis
12	3.2205	167.34	13.5	37.0	-19.5	lateralorbitofrontal
13	3.2088	319.11	6.5	-76.7	-0.8	lingual
14	-3.1768	49.43	11.2	-63.7	61.2	superiorparietal
15	-3.1348	63.97	38.3	-33.4	53.9	postcentral
16	-2.9896	25.80	47.5	33.5	-12.	parsorbitalis
17	-2.8765	100.05	44.4	-69.0	6.1	inferiorparietal
18	2.8507	60.53	19.1	-97.1	-13.3	lateraloccipital
19	-2.7798	88.59	6.9	-23.0	55.4	paracentral
20	-2.7326	26.22	6.6	-50.4	19.8	isthmuscingulate
Left hemisphere						
1	-5.4614	192.61	-57.3	-0.5	28.8	precentral
2	-6.7544	273.72	-57.0	44.1	32.6	supramarginal
3	-3.7923	18.66	-52.5	-19.3	52.6	postcentral

4	-3.7650	50.19	-39.4	4.2	51.6	caudalmiddlefrontal
5	-3.5873	20.10	-6.4	42.7	45.4	superiorfrontal

Figure Legends:

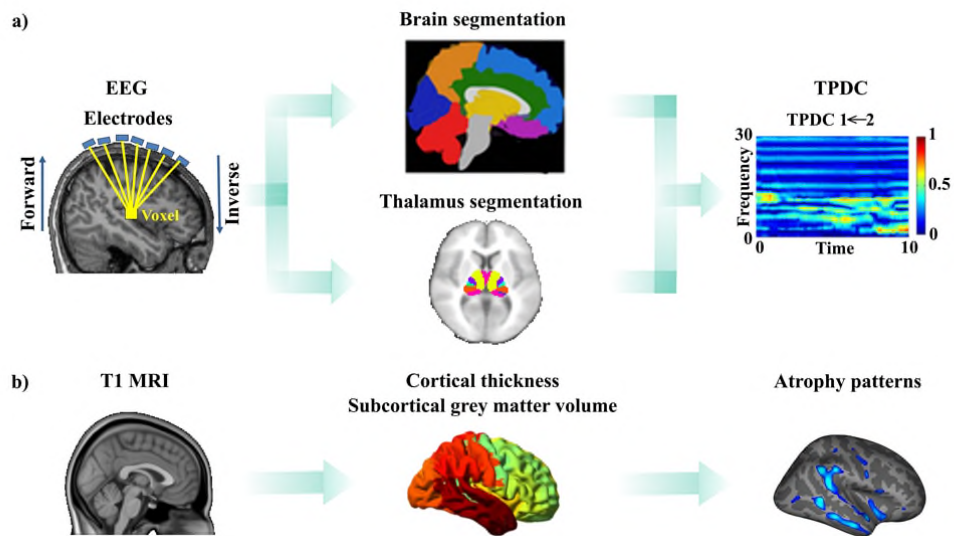


Figure 1. Overview of the analysis pipeline: **a)** electroencephalography (**EEG**) processing stream; **b)** magnetic resonance imaging (**MRI**) processing stream. **TPDC**: time-resolved partial directed coherence.

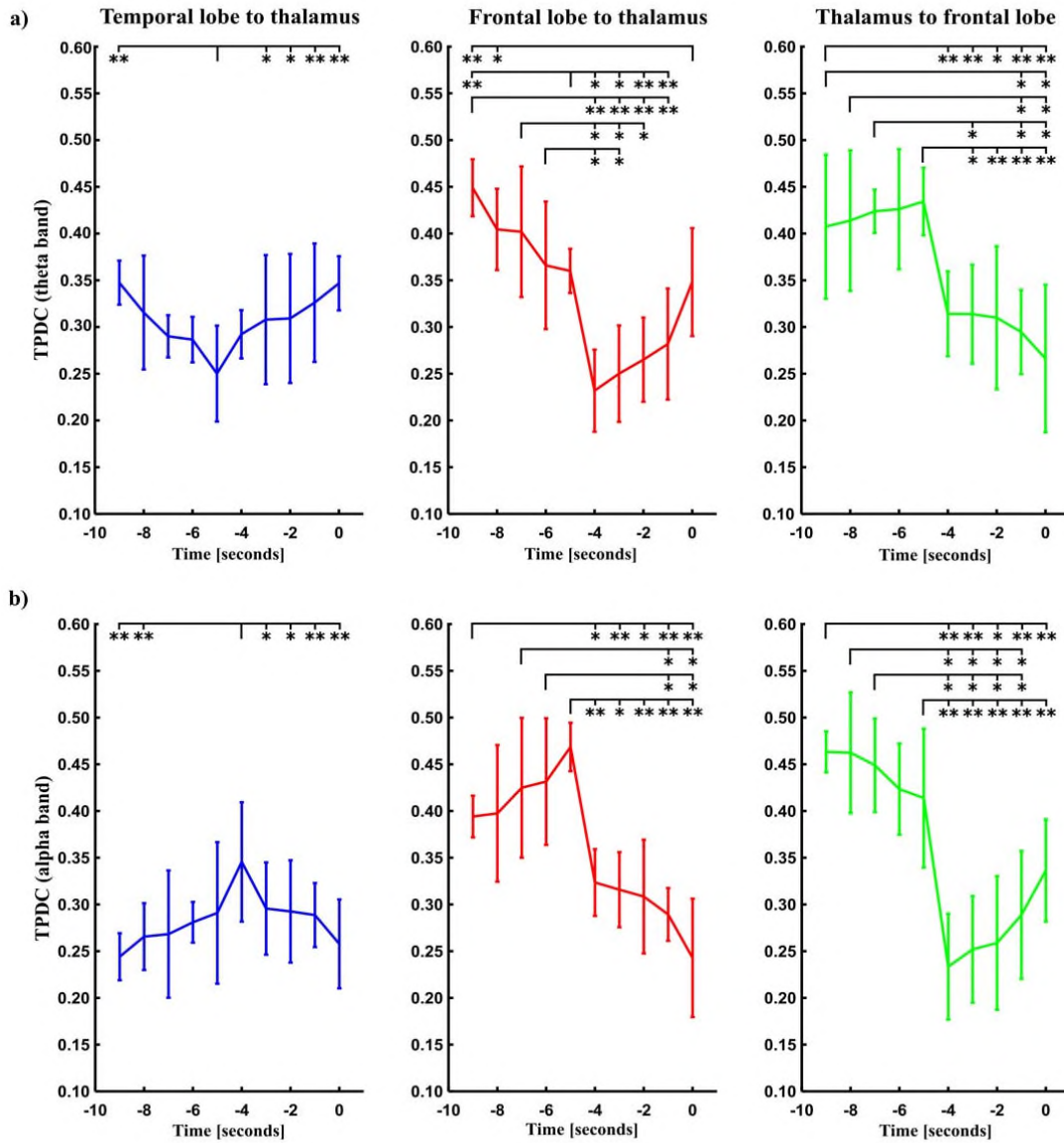


Figure 2. Temporal dynamics of effective connectivity in theta (a) and alpha (b) frequency bands. Connectivity breakdown between 4 and 5 seconds before the spike in reciprocal interconnections from frontal lobe to thalamus and from thalamus to frontal lobe. Significant changes of information flows at $*p < 0.001$, $**p < 0.0001$. **TPDC:** time-resolved partial directed coherence.

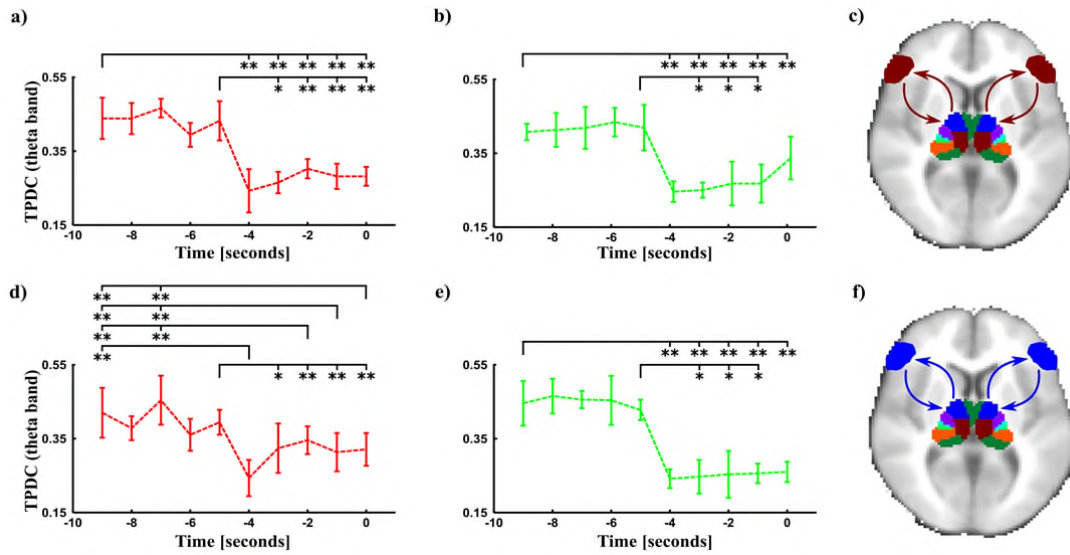


Figure 3. Connectivity dynamics in theta frequency band from frontal lobe to medial dorsal nucleus of thalamus (**a**) and vice versa (**b**) and from frontal lobe to ventral anterior nucleus of thalamus (**d**) and vice versa (**e**). Connectivity breakdown between 4 and 5 seconds before the spike ($*p < 0.001$, $**p < 0.0001$). Reciprocal flows between frontal lobe and medial dorsal nucleus (brown colored structures) (**c**) and between frontal lobe and ventral anterior nucleus (blue colored structures) (**f**) of thalamus. **TPDC**: time-resolved partial directed coherence.

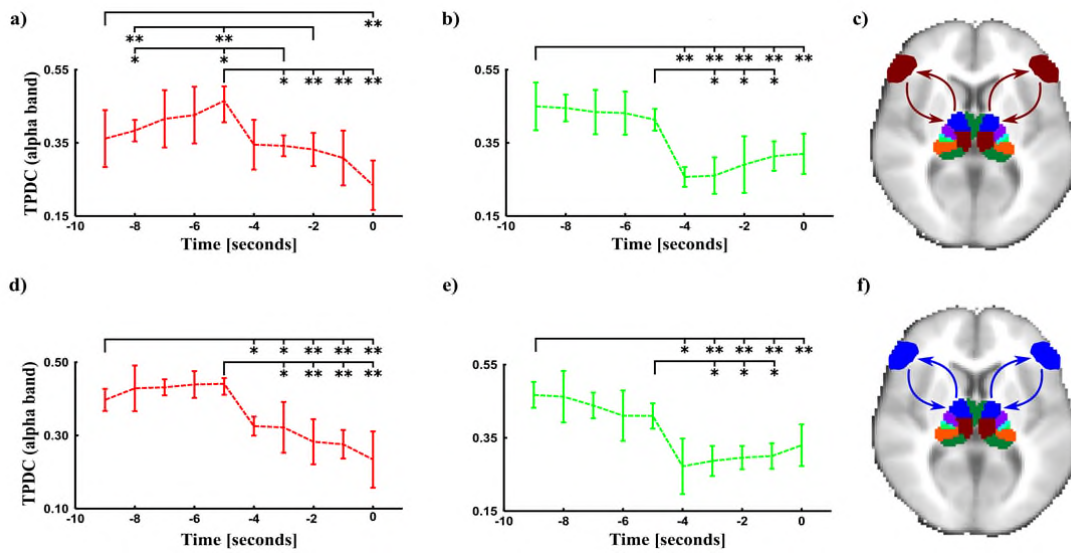


Figure 4. Connectivity dynamics in alpha frequency band from frontal lobe to medial dorsal nucleus of thalamus **(a)** and vice versa **(b)** and from frontal lobe to ventral anterior nucleus of thalamus **(d)** and vice versa **(e)**. Connectivity breakdown between 4 and 5 seconds before the spike ($*p < 0.001$, $**p < 0.0001$). Reciprocal flows between frontal lobe and medial dorsal nucleus (brown colored structures) **(c)** and between frontal lobe and ventral anterior nucleus (blue colored structures) **(f)** of thalamus. **TPDC:** time-resolved partial directed coherence.

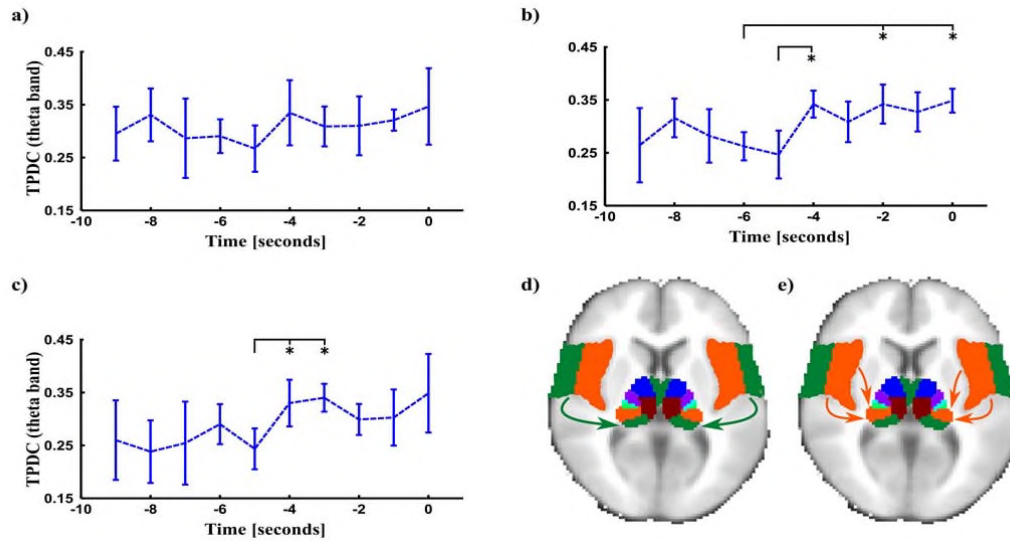


Figure 5. Effective connectivity dynamics in theta frequency band from temporal lobe towards anterior (a), lateral (b) and inferior (c) nuclei of pulvinar of thalamus. Directional flows from temporal lobe towards lateral and inferior (green colored structures) (d) and anterior (orange colored structures) (e) pulvinar nuclei of thalamus. ($*p < 0.0001$). TPDC: time-resolved partial directed coherence.

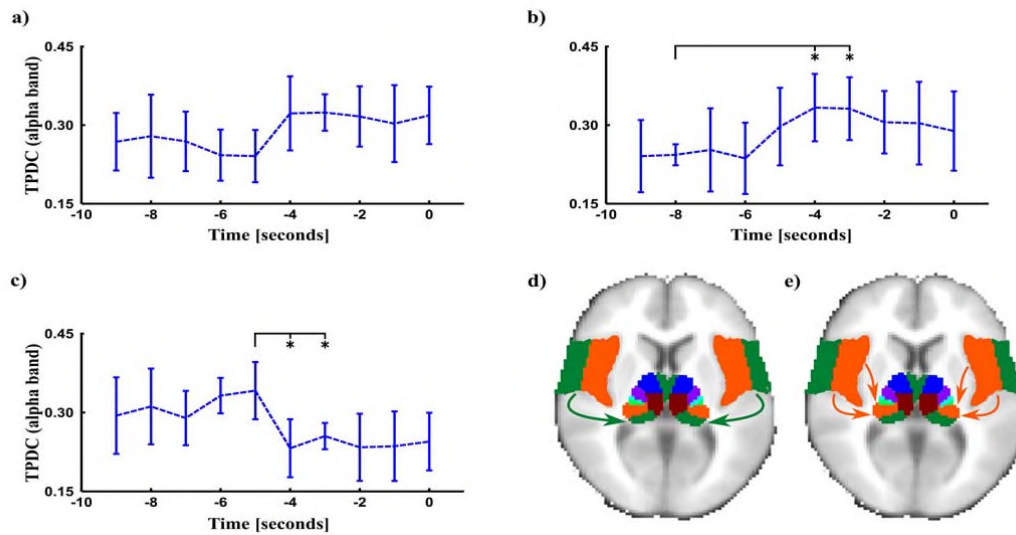


Figure 6. Effective connectivity dynamics in alpha frequency band from temporal lobe towards anterior (a), lateral (b) and inferior (c) nuclei of pulvinar of thalamus. Directional flows from temporal lobe towards lateral and inferior (green colored structures) (d) and anterior (orange colored structures) (e) pulvinar nuclei of thalamus. ($*p < 0.0001$). **TPDC:** time-resolved partial directed coherence.

a) Right hemisphere

b) Left hemisphere

34

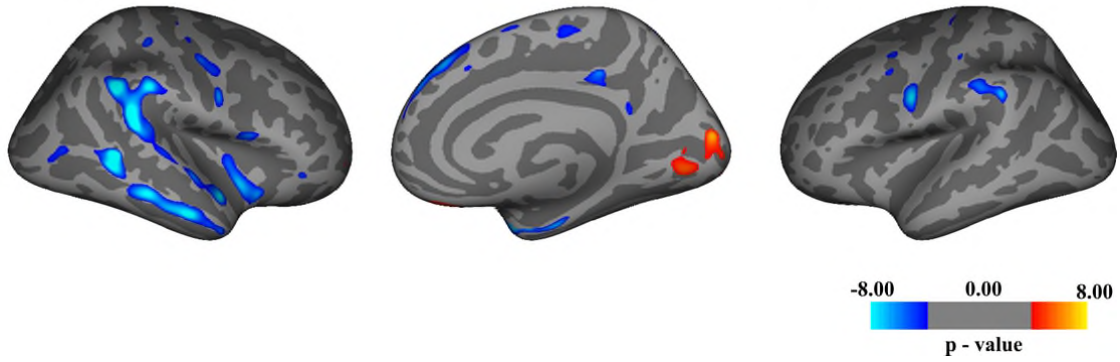


Figure 7. Statistical maps showing clusters ($p < 0.05$, FDR corrected) of cortical thinning (blue) and thickening (red) in epilepsy patients compared to healthy subjects. The two slices in **a)** show the regions in right hemisphere and **b)** shows in the left hemisphere. **FDR:** False Discovery Rate.